J|A|C|S
ARTICLES
Published on Web 11/26/2003

# Variable Coordination Geometries at the Diiron(II) Active Site of Ribonucleotide Reductase R2

Walter C. Voegtli,[†] Monika Sommerhalter,[†] Lana Saleh,[‡] Jeffrey Baldwin,[‡] J. Martin Bollinger, Jr.,*[,‡] and Amy C. Rosenzweig*[,†]

*Contribution from the Departments of Biochemistry, Molecular Biology, and Cell Biology and of Chemistry, Northwestern University, Evanston, Illinois 60208 and the Department of Biochemistry and Molecular Biology, The Pennsylvania State University, University Park, Pennsylvania 16802*

Received July 2, 2003; E-mail: jmb21@psu.edu; amyr@northwestern.edu

***Abstract:*** The R2 subunit of *Escherichia coli* ribonucleotide reductase contains a dinuclear iron center that generates a catalytically essential stable tyrosyl radical by one electron oxidation of a nearby tyrosine residue. After acquisition of Fe(II) ions by the apo protein, the resulting diiron(II) center reacts with $O_2$ to initiate formation of the radical. Knowledge of the structure of the reactant diiron(II) form of R2 is a prerequisite for a detailed understanding of the $O_2$ activation mechanism. Whereas kinetic and spectroscopic studies of the reaction have generally been conducted at pH 7.6 with reactant produced by the addition of Fe(II) ions to the apo protein, the available crystal structures of diferrous R2 have been obtained by chemical or photoreduction of the oxidized diiron(III) protein at pH 5−6. To address this discrepancy, we have generated the diiron(II) states of wildtype R2 (R2-wt), R2-D84E, and R2-D84E/W48F by infusion of Fe(II) ions into crystals of the apo proteins at neutral pH. The structures of diferrous R2-wt and R2-D48E determined from these crystals reveal diiron(II) centers with active site geometries that differ significantly from those observed in either chemically or photoreduced crystals. Structures of R2-wt and R2-D48E/W48F determined at both neutral and low pH are very similar, suggesting that the differences are not due solely to pH effects. The structures of these "ferrous soaked" forms are more consistent with circular dichroism (CD) and magnetic circular dichroism (MCD) spectroscopic data and provide alternate starting points for consideration of possible $O_2$ activation mechanisms.

## Introduction

Ribonucleotide reductase protein R2,[1] soluble methane monooxygenase hydroxylase (MMOH), and stearoyl acyl carrier protein $\Delta^9$ desaturase ($\Delta$9D) use diiron(II) centers to activate $O_2$ for difficult oxidation reactions and are members of the diiron−carboxylate family of oxidases and oxygenases.[2] In each of these proteins, the two iron ions are coordinated by two histidine and four carboxylate ligands, and the diiron cluster is housed in a four-helix bundle.[3] Despite these structural similarities, the ultimate outcome of the $O_2$ reaction is different for each system. In R2, reaction with $O_2$ leads to formation of a tyrosyl radical by the one-electron oxidation of an endogenous tyrosine residue.[4] The tyrosyl radical is essential for reduction of ribonucleotides to deoxyribonucleotides by the ribonucleotide reductase R1 subunit. By contrast, MMOH and $\Delta$9D catalyze two-electron oxidations. The reactions of $O_2$ with the diiron(II) centers in these enzymes result in oxidation of methane to methanol[5] and insertion of a double bond into stearic acid bound as a thioester to acyl carrier protein,[6] respectively.

Extensive spectroscopic and kinetic studies have provided insight into the mechanisms of these reactions. In MMOH, two intermediates, each more oxidized than the product diiron(III) cluster by two electrons, have been identified. The first to accumulate is a putative $\mu$-1,2-peroxodiiron(III) intermediate, **P** (or $\mathbf{H_{peroxo}}$). It decays to a formally $Fe(IV)_2$ cluster, **Q**, which is responsible for methane oxidation.[7−14] A $\mu$-1,2-peroxodiiron-

[†] Departments of Biochemistry, Molecular Biology, and Cell Biology and of Chemistry, Northwestern University.

[‡] Department of Biochemistry and Molecular Biology, The Pennsylvania State University.

(1) Abbreviations used: R2, R2 subunit of ribonucleotide reductase; MMOH, soluble methane monooxygenase hydroxylase; $\Delta$9D, stearoyl acyl carrier protein $\Delta^9$ desaturase; R2-wt, wildtype R2; R2-D84E, D84E mutant of ribonucleotide reductase R2 subunit; R2-D84E/W48F, D84E and W48F double mutant of ribonucleotide reductase R2 subunit; CD, circular dichroism; MCD, magnetic circular dichroism; EMTS, ethylmercurithiosalicylate.

(2) Solomon, E. I.; Brunold, T. C.; Davis, M. I.; Kemsley, J. N.; Lee, S.-K.; Lehnert, N.; Neese, F.; Skulan, A.; Yang, Y.-S.; Zhou, J. *Chem. Rev.* **2000**, *100*, 235−349.
(3) Nordlund, P.; Eklund, H. *Curr. Op. Struct. Biol.* **1995**, *5*, 758−766.
(4) Eklund, H.; Uhlin, U.; Färnegårdh, M.; Logan, D. T.; Nordlund, P. *Prog. Biophys. Mol. Biol.* **2001**, *77*, 177−268.
(5) Merkx, M.; Kopp, D. A.; Sazinsky, M. H.; Blazyk, J. L.; Müller, J.; Lippard, S. J. *Angew. Chem., Int. Ed.* **2001**, *40*, 2782−2807.
(6) Shanklin, J.; Cahoon, E. B. *Annu. Rev. Plant Physiol. Plant Mol. Biol.* **1998**, *49*, 611−641.
(7) Lee, S.-K.; Nesheim, J. C.; Lipscomb, J. D. *J. Biol. Chem.* **1993**, *268*, 21 569−21 577.
(8) Lee, S.-K.; Fox, B. G.; Froland, W. A.; Lipscomb, J. D.; Münck, E. *J. Am. Chem. Soc.* **1993**, *115*, 6450−6451.
(9) Liu, K. E.; Wang, D.; Huynh, B. H.; Edmondson, D. E.; Salifoglou, A.; Lippard, S. J. *J. Am. Chem. Soc.* **1994**, *116*, 7465−7466.
(10) Liu, K. E.; Valentine, A. M.; Wang, D.; Huynh, B. H.; Edmondson, D. E.; Salifoglou, A.; Lippard, S. J. *J. Am. Chem. Soc.* **1995**, *117*, 10 174−10 185.
(11) Shu, L.; Nesheim, J. C.; Kauffmann, K.; Münck, E.; Lipscomb, J. D.; Que, L., Jr. *Science* **1997**, *275*, 515−518.


**10.1021/ja0370387 CCC: $25.00** 

(III) adduct is also formed upon reaction of chemically reduced Δ9D with $O_2$.[15,16] In the reaction of *E. coli* R2, rapid injection of an "extra" electron prevents accumulation of two-electrons-oxidized diiron species and leads to formation of the Fe(IV)-Fe(III) cluster, **X**.[17−21] The electron is donated by a surface tryptophan residue, Trp 48, which forms a transient tryptophan cation radical. In the presence of reductant, the Trp 48 radical is then reduced, and **X** generates the catalytically essential tyrosyl radical by one-electron oxidation of Tyr 122.[22,23] Although species analogous to MMOH **P** and **Q** have not been observed in the reaction of R2-wt, a peroxo intermediate does accumulate in variants with iron ligand Asp 84 replaced by glutamic acid, a substitution that renders the ligand set identical to those in MMOH and Δ9D. This $\mu$-1,2-peroxodiiron(III) intermediate has been characterized in both the R2-D84E and R2-D84E/W48F variants.[24,25]

Numerous crystal structures of *E. coli* R2[26−31] and MMOH[32−34] in both the diiron(III) and diiron(II) states have been reported. In addition, the structure of diferrous Δ9D has been determined.[35] Technical obstacles have thus far precluded direct structural characterization of the reactive intermediates, but structural models have been obtained by computational methods.[36−40] In these studies, structures of diferrous R2 and MMOH have generally been invoked as starting points for evaluation of possible mechanistic pathways. The assumption that these crystal structures represent the $O_2$-reactive species in solution is not necessarily valid, however. In the case of MMOH, component B is required for $O_2$ reactivity and is known to affect the coordination of the diiron cluster.[5] The more appropriate starting diiron(II) cluster would be that in the MMOH·B complex, but the structure of this complex has not been determined. Different complications exist for R2. Although the diferrous form of this protein is, by itself, competent to react with $O_2$, kinetic and spectroscopic studies to detect and characterize intermediates have typically been conducted with reactant prepared by addition of ferrous ions to the apo protein at pH 7.6, whereas the available structures of diferrous *E. coli* R2-wt were all obtained by crystallization of the diiron(III) protein at pH 6 and either chemical or photoreduction at a pH between 5 and 6.[28] The discrepancy between the Fe(II) coordination numbers deduced by X-ray crystallography (two very similar four-coordinate Fe(II) sites) and circular dichroism (CD) and magnetic circular dichroism (MCD) spectroscopies (one four-coordinate and one five-coordinate Fe(II) site)[41] underscores the possibility that the geometry of the $O_2$-reactive diiron(II) cluster in R2 is significantly different from that seen in the crystal structures.

To address this possibility, we have developed an alternative procedure for generating the diiron(II) state in *E. coli* R2 crystals. This method involves soaking crystals of apo protein in solutions of ferrous ammonium sulfate and can be conducted at neutral pH. Surprisingly, crystals subjected to this treatment yielded structures with diiron centers different from those reported previously for diferrous R2-wt[28] and diferrous R2-D84E.[30] Structures of R2-wt and R2-D84E/W48F determined at both neutral and low pH suggest that the observed differences are probably not attributable to pH effects. The new structures are more consistent with the aforementioned CD/MCD spectroscopic data[41] and provide alternate starting points for consideration of the $O_2$ activation mechanism.

## Experimental Section

**Crystal Preparation.** Samples of R2-wt, R2-D84E, and R2-D84E/W48F were purified as described previously.[25,30,42] Purified material was diluted to 10 mg/mL in 100 mM HEPES pH 7.6, containing 1 mM sodium ethylmercurithiosalicylate (EMTS). Crystals of the apo proteins were grown by the hanging drop method in sealed Petri dishes at 37 °C.[30,43] Each drop contained 5 $\mu$L of protein and 5 $\mu$L of a precipitant solution consisting of 50 mM MES pH 6.0, 20% w/v PEG 4000, 200 mM NaCl, 1 mM EMTS, and 0.5% w/v dioxane. The crystals used for the structure determinations of "ferrous soaked" R2-wt, R2-D84E, and R2-D84E/W48F at neutral pH were prepared using the following method. Crystals were first transferred to 20 $\mu$L of a cryosolution containing 100 mM HEPES pH 7.5, 200 mM NaCl, 20% w/v PEG 4000, and 20% v/v glycerol at room temperature. After equilibration for 5 min, an equal volume of iron-loaded cryosolution containing 10 mM ferrous ammonium sulfate, 5 mN sulfuric acid, 200 mM NaCl, 20% w/v PEG 4000, and 20% v/v glycerol was added. The two cryosolutions were mixed first with a pipet tip and then with a large rayon loop. The final pH of the mixed cryosolution was measured to be 7.3. After soaking for 15 s to 2 min, crystals were mounted on

(12) Valentine, A. M.; Stahl, S. S.; Lippard, S. J. *J. Am. Chem. Soc.* **1999**, *121*, 3876−3887.
(13) Lee, S.-K.; Lipscomb, J. D. *Biochem.* **1999**, *38*, 4423−4432.
(14) Brazeau, B. J.; Lipscomb, J. D. *Biochem.* **2000**, *39*, 13 503−13 515.
(15) Broadwater, J. A.; Ai, J.; Loehr, T. M.; Sanders-Loehr, J.; Fox, B. G. *Biochem.* **1998**, *37*, 14 664−14 671.
(16) Broadwater, J.; Achim, C.; Munck, E.; Fox, B. G. *Biochem.* **1999**, *38*, 12 197−12 204.
(17) Bollinger, J. M., Jr.; Edmondson, D. E.; Huynh, H.; Filley, J.; Norton, J. R.; Stubbe, J. *Science* **1991**, *253*, 292−298.
(18) Tong, W. H.; Chen, S.; Lloyd, S. G.; Edmondson, D. E.; Huynh, B. H.; Stubbe, J. *J. Am. Chem. Soc.* **1996**, *118*, 2107−2108.
(19) Sturgeon, B. E.; Burdi, D.; Chen, S.; Huynh, B.-H.; Edmondson, D. E.; Stubbe, J.; Hoffman, B. H. *J. Am. Chem. Soc.* **1996**, *118*, 7551−7557.
(20) Willems, J. P.; Lee, H.-I.; Burdi, D.; Doan, P. E.; Stubbe, J.; Hoffman, B. M. *J. Am. Chem. Soc.* **1997**, *119*, 9816−9824.
(21) Riggs-Gelasco, P. J.; Shu, L.; Chen, S.; Burdi, D.; Huynh, B. H.; Que, L., Jr.; Stubbe, J. *J. Am. Chem. Soc.* **1998**, *120*, 849−860.
(22) Baldwin, J.; Krebs, C.; Ley, B. A.; Edmondson, D. E.; Huynh, B. H.; Bollinger, J. M., Jr. *J. Am. Chem. Soc.* **2000**, *122*, 13 195−13 206.
(23) Krebs, C.; Chen, S.; Baldwin, J.; Ley, B. A.; Patel, U.; Edmondson, D. E.; Huynh, B. H.; Bollinger, J. M., Jr. *J. Am. Chem. Soc.* **2000**, *122*, 12 207−12 219.
(24) Bollinger, J. M., Jr.; Krebs, C.; Vicol, A.; Chen, S.; Ley, B. A.; Edmondson, D. E.; Huynh, B. H. *J. Am. Chem. Soc.* **1998**, *120*, 1094−1095.
(25) Moënne-Loccoz, P.; Baldwin, J.; Ley, B. A.; Loehr, T. M.; Bollinger, J. M., Jr. *Biochem.* **1998**, *37*, 14 659−14 663.
(26) Nordlund, P.; Sjöberg, B.-M.; Eklund, H. *Nature* **1990**, *345*, 593−598.
(27) Nordlund, P.; Eklund, H. *J. Mol. Biol.* **1993**, *231*, 123−164.
(28) Logan, D. T.; Su, X.-D.; Åberg, A.; Regnström, K.; Hajdu, J.; Eklund, H.; Nordlund, P. *Structure* **1996**, *4*, 1053−1064.
(29) Andersson, M. E.; Högbom, M.; Rinaldo-Matthis, A.; Andersson, K. K.; Sjöberg, B.-M.; Nordlund, P. *J. Am. Chem. Soc.* **1999**, *121*, 2346−2352.
(30) Voegtli, W. C.; Khidekel, N.; Baldwin, J.; Ley, B. A.; Bollinger, J. M., Jr.; Rosenzweig, A. C. *J. Am. Chem. Soc.* **2000**, *122*, 3255−3261.
(31) Baldwin, J.; Voegtli, W. C.; Khidekel, N.; Moënne-Loccoz, P.; Krebs, C.; Pereira, A. S.; Ley, B. A.; Huynh, B. H.; Loehr, T. M.; Riggs-Gelasco, P. J.; Rosenzweig, A. C.; Bollinger, J. M., Jr. *J. Am. Chem. Soc.* **2001**, *123*, 7017−7030.
(32) Rosenzweig, A. C.; Frederick, C. A.; Lippard, S. J.; Nordlund, P. *Nature* **1993**, *366*, 537−543.
(33) Rosenzweig, A. C.; Nordlund, P.; Takahara, P. M.; Frederick, C. A.; Lippard, S. J. *Chem. Biol.* **1995**, *2*, 409−418.
(34) Whittington, D. A.; Lippard, S. J. *J. Am. Chem. Soc.* **2001**, *123*, 827−838.
(35) Lindqvist, Y.; Huang, W.; Schneider, G.; Shanklin, J. *EMBO J.* **1996**, *15*, 4081−4092.
(36) Torrent, M.; Musaev, D. G.; Basch, H.; Morokuma, K. *J. Comput. Chem.* **2002**, *23*, 59−76.
(37) Dunietz, B. D.; Beachy, M. D.; Cao, Y.; Whittington, D. A.; Lippard, S. J.; Friesner, R. A. *J. Am. Chem. Soc.* **2000**, *122*, 2828−2839.
(38) Siegbahn, P. E. M. *Inorg. Chem.* **1999**, *38*, 2880−2889.
(39) Siegbahn, P. E. M.; Crabtree, R. H.; Nordlund, P. *J. Biol. Inorg. Chem.* **1998**, *3*, 314−317.
(40) Siegbahn, P. E. M.; Crabtree, R. H. *J. Am. Chem. Soc.* **1997**, *119*, 3103−3113.
(41) Pulver, S. C.; Tong, W. H.; Bollinger, J. M., Jr.; Stubbe, J.; Solomon, E. I. *J. Am. Chem. Soc.* **1995**, *117*, 12 664−12 678.
(42) Parkin, S. E.; Chen, S.; Ley, B. A.; Mangravite, L.; Edmondson, D. E.; Huynh, B. H.; Bollinger, J. M., Jr. *Biochem.* **1998**, *37*, 1124−1130.
(43) Nordlund, P.; Uhlin, U.; Westergren, C.; Joelson, T.; Sjöberg, B.-M.; Eklund, H. *FEBS Lett.* **1989**, *258*, 251−254.

***Table 1.*** Data Collection and Refinement Statistics

| | R2-wt pH 7 | R2-wt pH 5 | R2-D84E pH 7 | R2-D84E/W48F pH 7 | R2-D84E/W48F pH 5 | Mn R2-D84E pH 7 |
|---|---|---|---|---|---|---|
| | | | data collection[a] | | | |
| unit cell dimensions | | | | | | |
| *a* (Å) | 73.9 | 74.2 | 74.0 | 74.0 | 74.1 | 74.0 |
| *b* (Å) | 84.6 | 84.2 | 84.8 | 84.4 | 84.2 | 83.9 |
| *c* (Å) | 114.1 | 114.2 | 114.8 | 114.6 | 114.7 | 114.3 |
| resolution range (Å) | 25−1.68 | 50−1.95 | 25−1.90 | 25−1.90 | 25−1.95 | 50−1.80 |
| no. of total observations | 1 103 745 | 228 122 | 451 466 | 556 805 | 393 987 | 566 232 |
| no. of unique observations | 80 287 | 51 995 | 55 182 | 55 199 | 52 866 | 66 524 |
| completeness (%)[b] | 97.8 (93.0) | 99.6 (98.7) | 95.7 (90.7) | 98.1 (93.8) | 99.5 (99.7) | 99.8 (99.8) |
| $R_{sym}$[c] | 0.061 (0.391) | 0.108 (0.415) | 0.062 (0.240) | 0.066 (0.324) | 0.056 (0.276) | 0.060 (0.206) |
| I/$\sigma$ | 16.2 (2.1) | 16.2 (2.9) | 16.7 (2.4) | 16.4 (2.5) | 18.4 (4.1) | 8.0 (3.5) |
| | | | refinement | | | |
| resolution range (Å) | 25−1.68 | 25−1.95 | 20−1.90 | 25−1.90 | 25−1.95 | 25−1.80 |
| no. of reflections | 77 979 | 50 619 | 53 464 | 54 370 | 51 480 | 66 394 |
| *R*-factor[d] | 20.3 | 20.7 | 21.5 | 20.5 | 19.4 | 18.6 |
| *R*-free | 24.7 | 23.6 | 23.8 | 23.6 | 22.2 | 21.5 |
| no. of atoms | | | | | | |
| protein, nonhydrogen | 5570 | 5566 | 5572 | 5564 | 5566 | 5556 |
| nonprotein | 364 | 213 | 246 | 267 | 334 | 443 |
| rms bond length (Å) | 0.007 | 0.006 | 0.006 | 0.007 | 0.005 | 0.004 |
| rms bond angles (deg) | 1.2 | 1.1 | 1.1 | 1.1 | 1.0 | 1.0 |
| av *B* value (Å$^2$) | | | | | | |
| main chain | 18.8 | 33.0 | 18.8 | 22.3 | 25.0 | 19.8 |
| side chain | 25.4 | 37.1 | 20.1 | 23.8 | 28.7 | 23.1 |

[a] All data except for the R2-wt pH 5 data set were collected at −160 °C at Stanford Synchrotron Radiation Laboratory (SSRL). The R2-wt pH 7 and R2-D84E/W48F pH 7 data sets were collected at beamline 9−1 ($\lambda$ = 0.97 Å), the R2-D84E data set was collected at beamline 9−1 ($\lambda$ = 0.946 Å), the R2-D84E/W48F pH 5 data set was collected at beamline 7−1 ($\lambda$ = 1.08 Å), and the Mn R2-D84E data set was collected at beamline 9−2 ($\lambda$ = 1.28 Å). The R2-wt pH 5 data set was collected at beamline 8.2.2 ($\lambda$ = 1.078 Å) at the Advanced Light Source (ALS). [b] Values in parentheses are for the highest resolution shells. [c] $R_{sym} = \Sigma|I_{obs} - I_{avg}|/\Sigma I_{obs}$, where the summation is over all reflections. [d] *R*-factor $= \Sigma|F_{obs} - F_{calc}|/\Sigma F_{obs}$. Test set sizes: 5.0% for R2-wt pH 7 and 10% for R2-wt pH 5, 4.7% for R2-D84E, 4.8% for both R2-D84E/W48F structures, and 10% for Mn R2-D84E.

rayon loops and frozen in liquid nitrogen. The crystals used for the structure determinations of ferrous soaked R2-wt and R2-D84E/W48F at low pH were prepared by a similar procedure except that 50 mM ferrous ammonium sulfate was used, resulting in a final pH of 5. The crystal used for the structure determination of Mn-substituted R2-D84E was soaked for 10 min in 100 mM HEPES pH 7.5, 200 mM NaCl, 20% w/v PEG 4000, and 20% v/v glycerol, supplemented with 10 mM $MnCl_2$.

**Data Collection and Refinement.** X-ray diffraction data were collected at −160 °C at Stanford Synchrotron Radiation Laboratory (SSRL). Data were integrated with DENZO[44] or MOSFLM[45] and scaled with SCALEPACK[44] or SCALA[46] (Table 1). The structures were solved by molecular replacement with CNS[47] using the structure of dithionite-reduced R2-D84E[30] without solvent molecules or iron ions as a starting model. Initial rigid body refinement to 3.0 Å resolution was followed by iterative cycles of energy minimization, simulated annealing, restrained individual B-factor refinement, and model rebuilding with the programs O[48] and XtalView.[49] The positions of the metal ions were determined from $F_o-F_c$ difference electron density maps calculated after the first complete round of refinement, and Lennard−Jones parameters for Fe(II) and Mn(II)[47] were used. Lowering the iron occupancies for any of the four sites below 100% produced positive peaks in $F_o-F_c$ difference maps, suggesting that all iron sites are fully occupied. The four manganese sites are all >90% occupied. Solvent molecules placed at peaks >3.0$\sigma$ in $F_o-F_c$ difference electron density maps were retained if their B-values refined to <60 Å$^2$. For the structure of ferrous soaked R2-wt, a final refinement cycle with SHELX was performed.[50] Ramachandran plots generated with PROCHECK indicate that the six models exhibit good geometry with >99.7% of the residues in the most favored or additionally allowed regions. Figures were generated with MOLSCRIPT,[51] BOBSCRIPT,[52] and RASTER3D.[53] The coordinates for ferrous soaked R2-wt at pH 7.3, R2-wt at pH 5, R2-D84E, R2-D84E/W48F at pH 7.3, R2-D84E/W48F at pH 5, and manganese soaked R2-D84E have been deposited in the Protein Data Bank with accession codes 1PIY, 1R65, 1PIZ, 1PJ0, 1PJ1, and 1PM2, respectively.

## Results

**Structure of Ferrous Soaked R2-wt at pH 7.3 and at pH 5.** Soaking ferrous ions into a crystal of apo R2-wt at pH 7.3 resulted in the formation of the diiron cluster shown in Figures 1A, 1B, and 2A. The similarity of the soaking procedure to well-established procedures for generating the $O_2$-reactive diiron(II) state in solution[18,22,42,54] and aspects of the final structural model indicate that the cluster is reduced. Specifically, the absence of any exogenous ligands coordinated to the iron ions and the long Fe···Fe distance of 3.8 Å (Figure 2A) are most consistent with a diiron(II) site. Comparison of this structure, designated ferrous soaked R2-wt, with that of reduced R2 obtained either by treatment with dithionite and phenosafranin or by X-ray photoreduction in the synchrotron beam[28] (Figure 1D) reveals both similarities and differences. In both structures, Glu 115 bridges the two Fe(II) ions in a $\mu$-1,3 fashion and each Fe(II) ion is coordinated by the $\delta$ nitrogen of a

(44) Otwinowski, Z.; Minor, W. *Methods Enzymol.* **1997**, *276*, 307−326.
(45) Leslie, A. G. W. *Joint CCP4 + ESF-EAMCB Newsletter on Protein Crystallography* **1992**, *26*.
(46) Collaborative Computational Project Number 4. *Acta Crystallogr.* **1994**, *D50*, 760−763.
(47) Brünger, A. T.; Adams, P. D.; Clore, G. M.; DeLano, W. L.; Gros, P.; Grosse-Kunstleve, R. W.; Jiang, J.-S.; Kuszewski, J.; Nilges, M.; Pannu, N. S.; Read, R. J.; Rice, L. M.; Simonson, T.; Warren, G. L. *Acta Crystallogr.* **1998**, *D54*, 905−921.
(48) Jones, T. A.; Zou, J.-Y.; Cowan, S. W.; Kjeldgaard, M. *Acta Crystallogr.* **1991**, *A47*, 110−119.
(49) McRee, D. E. *J. Struct. Biol.* **1999**, *125*, 156−165.
(50) Sheldrick, G. M.; Schneider, T. R. *Methods Enzymol.* **1997**, *277*, 319−343.
(51) Kraulis, P. J. *J Appl. Crystallogr.* **1991**, *24*, 946−950.
(52) Esnouf, R. M. *J. Mol. Graph. Model.* **1997**, *15*, 132−134.
(53) Merritt, E. A.; Bacon, D. J. *Methods Enzymol.* **1997**, *277*, 505−524.
(54) McCormick, J. M.; Reem, R. C.; Foroughi, J.; Bollinger, J. M.; Jensen, G. M.; Stephens, P. J.; Stubbe, J.; Solomon, E. I. *New J. Chem.* **1991**, *15*, 439−444.

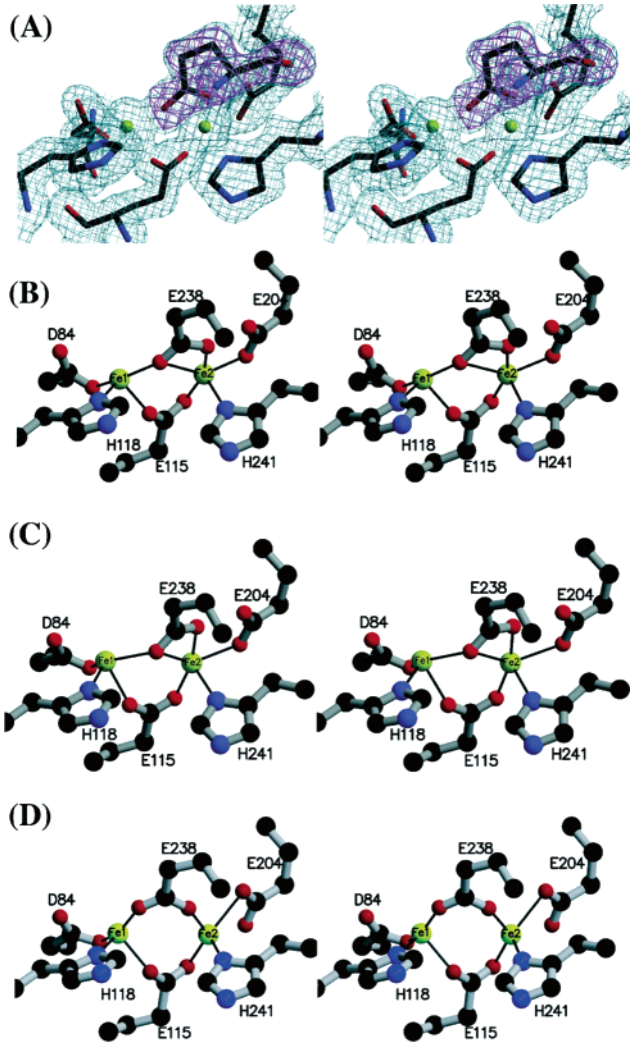


***Figure 1.*** Diiron center in diferrous R2-wt. (A) Final $2F_o-F_c$ electron density map (contoured at $1\sigma$, light blue) at the diiron center in ferrous soaked R2-wt. An $F_o-F_c$ simulated annealing omit map with Glu 238 omitted is superimposed (contoured at $4.5\sigma$, magenta). (B) Stereo ball-and-stick representation of the diiron center in ferrous soaked R2-wt at pH 7.3. (C) Stereo ball-and-stick representation of the diiron center in ferrous soaked R2-wt at pH 5. (D) Stereo ball-and-stick representation of the diiron center in photoreduced R2-wt (PDB accession code 1XIK).

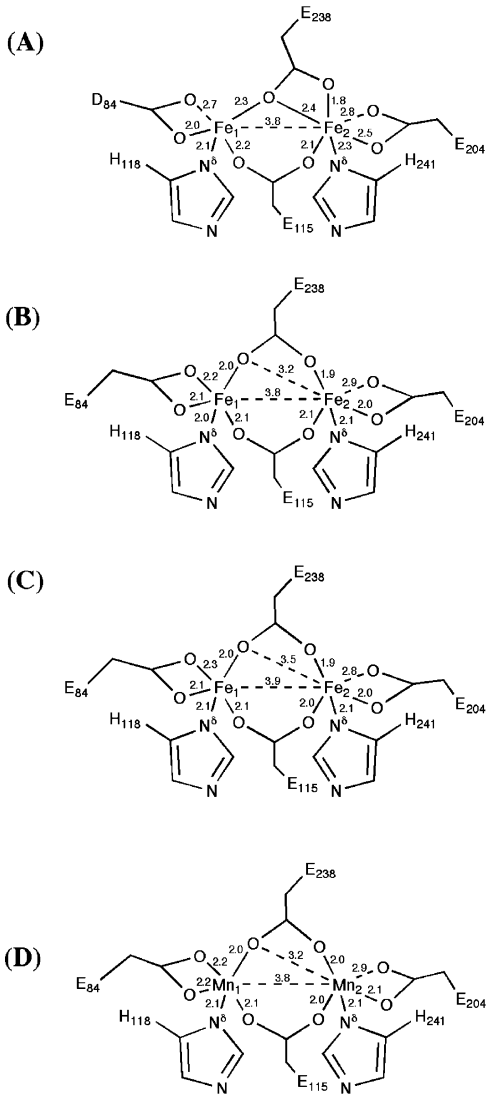


***Figure 2.*** Schematic diagrams of the metal coordination at pH 7.3 in ferrous soaked (A) R2-wt, (B) R2-D84E, (C) R2-D84E/W48F, and in (D) Mn-substituted R2-D84E. Interatomic distances are shown in Å and represent an average over the two monomers in the R2 dimer. In all four structures, the coordination geometry is the same in both monomers.

histidine. The average Fe1···O distances for the two side chain oxygen atoms of Asp 84 are 2.0 and 2.7 Å. It should be noted, however, that the position of the uncoordinated side chain oxygen atom differs between the two subunits, with Fe1···O distances of 3.0 Å in monomer A and 2.5 Å in monomer B. Because the electron density is better defined for monomer A, Asp 84 is best described as a monodentate, terminal ligand. Residue Glu 204 is a monodentate, terminal ligand to Fe2, although the average Fe2···O distance of 2.5 Å (2.6 Å in monomer A and 2.4 Å in monomer B), is somewhat long (Figure 2A). The corresponding average distance in the structure of the photoreduced protein is 2.3 Å.[28] The Glu 204 coordinated oxygen atom forms hydrogen bonds with the side chain nitrogen atoms of Gln 87 and Trp 111. Similar interactions are also present in the structure of the photoreduced protein, but in this case involve the uncoordinated oxygen atom of Glu 204.

The most important difference between the two structures is the position of Glu 238. In the dithionite-reduced and photoreduced forms, Glu 238 bridges the two iron ions in a $\mu$-1,3 fashion, but in the ferrous soaked protein, Glu 238 adopts a $\mu$-($\eta^1$,$\eta^2$) coordination mode with one oxygen atom bridging the two iron ions and both oxygen atoms coordinated to Fe2. As a result, Fe1 is four-coordinate and Fe2 is five-coordinate (Figure 1B). In the previously reported structures, both Fe(II) ions are four-coordinate (Figure 1D).[28] The two Glu 238 oxygen atoms chelate Fe2 in an asymmetric fashion with Fe···O distances of 2.4 Å for the bridging oxygen atom and 1.8 Å for the terminal oxygen atom (Figure 2A). The difference between these distances suggests a slight inclination toward $\mu$-1,3 geometry, but 2.4 Å is still sufficiently short to be considered as direct coordination. The analogous distance in the photoreduced protein is 3.3 Å averaged over the two monomers. The $\mu$-($\eta^1$,$\eta^2$) coordination mode of Glu238 has been observed previously in the azide adduct of dithionite-reduced R2-Y122F/F208A,[29] in dithionite-reduced R2-D84E,[30] and in the oxidized Mn-substituted R2.[55] In the dithionite-reduced R2-D84E cluster, the two oxygen atoms chelate Fe2 in a more symmetric fashion with both average Fe···O distances being 2.3 Å. The change in coordination geometry at Fe2 in the ferrous soaked protein does

not affect the Fe1 site. In particular, the average distance between Fe1 and the side chain oxygen of Tyr 122 is 4.8 Å in both the ferrous soaked and photoreduced proteins.

Soaking ferrous ions into crystals of apo R2-wt at pH 5 resulted in slightly different diiron(II) cluster structures for the two monomers in the R2 dimer. In monomer B (Figure 1C), the diiron(II) cluster closely resembles that obtained at pH 7.3 (Figure 1B). All of the bond distances are comparable, and Glu 238 adopts a $\mu$-($\eta^1$,$\eta^2$) coordination mode. This similarity suggests that the pH at which the crystals are soaked and frozen does not significantly affect the geometry of the active site, at least for monomer B. The geometry of the diiron(II) cluster in monomer A is more ambiguous, however. For Glu 238, the Fe2···O distance for the bridging oxygen atom is 2.8 Å. By contrast, the analogous distance in both monomer B and the pH 7 structure is 2.4 Å (Figure 2A). Although 2.8 Å is long for direct coordination and suggests a tendency toward $\mu$-1,3 coordination, it is substantially shorter than the average value of 3.3 Å observed in photoreduced R2. In addition, the equivalent distance in ferrous soaked R2-D84E and R2-D84E/W48F is 3.2−3.5 Å (vide infra, Figure 2B,C). Thus, the coordination mode of Glu 238 in monomer A is best described as intermediate between $\mu$-($\eta^1$,$\eta^2$) and $\mu$-1,3 geometry. Notably, this difference between the two monomers was observed reproducibly in two structures of R2-wt at pH 5.

**Structure of Ferrous Soaked R2-D84E at pH 7.3.** Soaking ferrous ions into a crystal of apo R2-D84E at neutral pH resulted in the diiron(II) cluster structure shown in Figures 3A,B and 2B. Comparison of this diiron(II) cluster to the R2-D84E diiron-(II) cluster generated by dithionite reduction of oxidized crystals at pH 5 (Figure 3C)[30] reveals several significant differences. First, the Fe···Fe distance is 3.9 Å, whereas the Fe···Fe distance in the dithionite-reduced protein is 3.5 Å. Second, Glu 238 bridges the diiron cluster in a $\mu$-1,3 fashion instead of the $\mu$-($\eta^1$,$\eta^2$) geometry observed in the dithionite-reduced form. Both the Fe···Fe distance and the orientation of Glu 238 are more similar to that observed in the dithionite and photoreduced R2-wt proteins (Figure 1C)[28] than in the dithionite-reduced R2-D84E protein (Figure 3C).[30] Third, Glu 204, which is a monodentate terminal ligand to Fe2, adopts a syn conformation in the ferrous soaked protein and an anti conformation in the dithionite-reduced form. The syn conformation is observed in all the R2-wt structures as well (Figure 1). As in the photoreduced R2-wt protein, the uncoordinated oxygen atom of Glu 204 interacts with Gln 87 and Trp 111. The analogous hydrogen bonds in the dithionite-reduced R2-D84E involve the coordinated oxygen atom. Finally, a solvent molecule coordinated to Fe2 in the dithionite-reduced protein is not present in the ferrous soaked protein. As a result of these changes, Fe1 is five-coordinate and Fe2 is four-coordinate. In both structures, Glu 84 is bidentate chelating to Fe1 and the distance between Fe1 and the side chain oxygen of Tyr 122 is longer than the ∼5 Å observed for diferrous R2-wt. The average distances are 6.2 and 6.7 Å for the dithionite-reduced and ferrous soaked proteins, respectively.

**Structure of Mn-Substituted R2-D84E at pH 7.5.** Soaking Mn(II) ions into crystals of R2-D84E at neutral pH resulted in the dimanganese(II) cluster structure shown in Figures 2D and 3D. The coordination geometry is very similar to that in ferrous soaked R2-D84E (Figures 2B, 3B). This structure differs from that of Mn-substituted R2-wt [55,56] in several ways. First, Glu 84 is chelating in Mn-substituted R2-D84E, but Asp 84 is a monodentate, terminal ligand in Mn-substituted R2-wt. Second, Glu 204 adopts an anti conformation in Mn-substituted R2-wt, but a syn conformation in Mn-substituted R2-D84E. Finally, a water molecule coordinated to Mn2 in Mn-substituted R2-wt is not present. The average distance between Mn1 and the side chain oxygen of Tyr 122 is 6.7 Å as compared to ∼5 Å in Mn-substituted R2-wt, consistent with what is observed for the diferrous forms of R2-D84E and R2-wt (regardless of how the diiron(II) cluster is generated). Although Mn-substituted R2-D84E and ferrous soaked R2-D84E are very similar, Mn-substituted R2-wt and ferrous soaked R2-wt differ, with Mn-substituted R2-wt more closely resembling chemically reduced R2-wt. This observation suggests that Mn(II) substituted diiron proteins might not always be valid models for the relevant diiron(II) proteins.

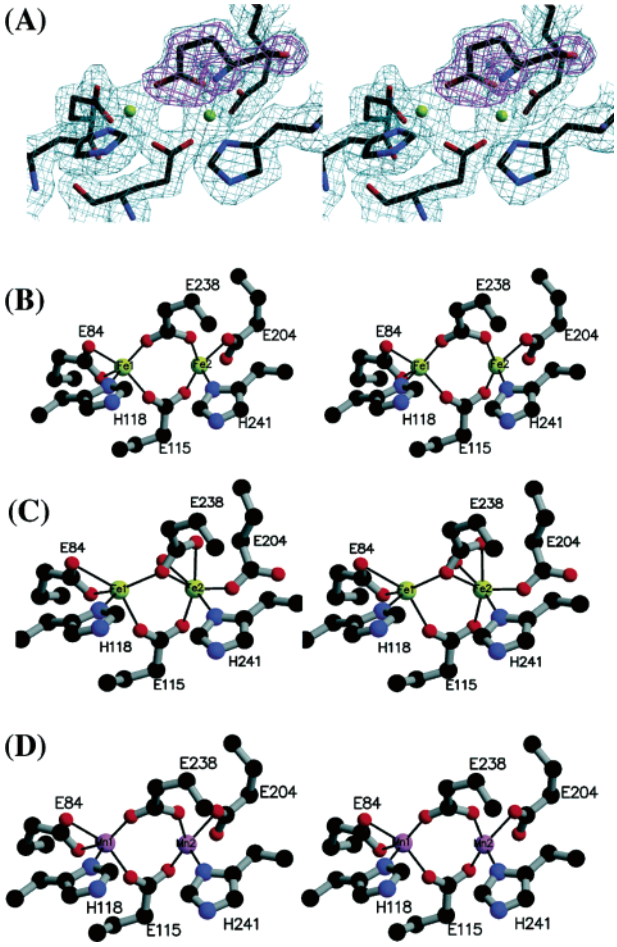


***Figure 3.*** Metal center center in R2-D84E. (A) Final $2F_o-F_c$ electron density map (contoured at 1$\sigma$, light blue) at the diiron center in ferrous soaked R2-D84E. An $F_o-F_c$ simulated annealing omit map with Glu 238 omitted is superimposed (contoured at 4.5$\sigma$, magenta). (B) Stereo ball-and-stick representation of the diiron center in ferrous soaked R2-D84E. (C) Stereo ball-and-stick representation of the diiron center in dithionite-reduced R2-D84E (PDB accession code 1PIM). A solvent molecule coordinated to Fe2 is shown as a red sphere. (D) Stereo ball-and-stick representation of the dimanganese center in Mn-substituted R2-D84E.

(55) Högbom, M.; Andersson, M. E.; Nordlund, P. *J. Biol. Inorg. Chem.* **2001**, *6*, 315−323.

(56) Atta, M.; Nordlund, P.; Aberg, A.; Eklund, H.; Fontecave, M. *J. Biol. Chem.* **1992**, *267*, 20 682−20 688.

**Structures of Ferrous Soaked R2-D84E/W48F at pH 7.3 and at pH 5.** The diiron(II) clusters of R2-D84E/W48F obtained by soaking ferrous ions into crystals of apo protein at pH 7.3 and pH 5 are nearly identical, with the same coordination geometry observed for all four monomers in the two structures-(Figure 2C). The similarity in coordination geometries and bond distances suggests that the pH at which the crystals are soaked and frozen does not affect the active site structure for this R2 variant. The details of coordination are the same as in the ferrous soaked form of R2-D84E (Figure 3B), indicating that the W48F mutation has little effect on the diiron cluster. In the structures of R2-wt and R2-D84E, the side chain nitrogen atom of Trp 48 is hydrogen bonded to a side chain oxygen atom of Asp 237 which, in turn, interacts with the $\epsilon$ nitrogen of Fe1 ligand His 118. Replacement of Trp 48 with phenylalanine eliminates the interaction between residue 48 and Asp 237, but Asp 237 and His 118 remain strongly hydrogen bonded, with an average distance of 2.6 Å. No exogenous Fe ligands are observed in R2-D84E/W48F at either pH.

## Discussion

**Relation between Coordination Geometry and the Method Used to Generate the Diiron(II) Cluster.** The diiron(II) center can be generated in crystals of *E. coli* R2 by three different techniques. First, Nordlund and co-workers fortuitously discovered that exposure of oxidized crystals to the synchrotron X-ray beam followed by annealing results in reduction to the diiron(II) form.[28] For both the *Salmonella typhimurium* R2[57] and the related Δ9D,[35] reduction occurred during exposure to the X-ray beam without thawing and refreezing of the crystal. Second, crystals of oxidized *E. coli* R2 can be chemically reduced by the addition of dithionite and phenosafranin. This procedure was used for previously reported structures of R2-wt,[28] R2-D84E,[30] and the azide complex of R2-Y122F/F208A.[29] Crystals of diferrous R2 from *Salmonella typhimurium*[57] were also obtained by chemical reduction. In the case of diferrous R2-wt from *E. coli*, chemical reduction and reduction by synchrotron radiation yielded the same coordination geometry at the diiron(II) center.[28]

The third method of producing the diiron(II) state in R2 crystals involves soaking crystals of apo protein in solutions of ferrous ammonium sulfate. Crystals of diferrous R2 from *Corynebacterium ammoniagenes* were prepared by soaking apo crystals in solutions of ferrous ammonium sulfate, dithionite, and phenosafranin.[58] In previous mechanistic studies, the $O_2$-reactive diiron(II) form of R2 has been prepared in solution either by addition of ferrous ammonium sulfate to apo protein[18,22] or by chemical reduction of the diiron(III) form followed by anaerobic removal of dithionite and phenosafranin.[30] Therefore, it might be expected that the same diiron(II) cluster structure would be obtained in crystals prepared by the two methods. Surprisingly, the structures of ferrous soaked R2-wt and R2-D84E presented here differ significantly from those obtained by chemical reduction. We considered the possibility that the observed differences are random and unrelated to the method used to generate the diiron(II) cluster, but the results are completely reproducible. The ferrous soaking experiment was performed on numerous crystals followed by data collection and independent refinement. Two structures of R2-wt at neutral pH, two structures of R2-wt at low pH, eight structures of R2-D84E, four structures of R2-D84E/W48F at neutral pH, and seven structures of R2-D84E/W48F at low pH were obtained. For each protein, the same coordination geometry was observed in every structure. Thus, the diiron(II) cluster coordination geometry clearly depends on the method used to prepare the crystals.

One difference between dithionite reduction of oxidized crystals and addition of ferrous ions to crystals of the apo protein is the pH at which the crystals are soaked and frozen. Treatment with ferrous ammonium sulfate was conducted at pH 7.3, whereas the pH of the soaking solution after chemical reduction was approximately 5.[28,30] Several considerations suggest that the observed variations in active site structure are not due solely to changes in pH. The structures of ferrous soaked R2-D84E/W48F determined from crystals prepared at pH 7.3 and pH 5 are indistinguishable (Figure 2C). In addition, the diiron(II) clusters in both monomers of ferrous soaked R2-wt at pH 7.3 (Figure 1B) and one monomer of ferrous soaked R2-wt at pH 5 (Figure 1C) are very similar. Finally, the structures of R2-wt obtained by dithionite reduction at pH ∼5 and photoreduction at pH 6.0 are virtually identical.[28] These similarities suggest that changes in pH over the range of 5 to 7 cannot be primarily responsible for the difference in coordination.

Another difference between the two procedures is the initial geometry of the active site. Whereas chemical reduction involves adding reductants to an already assembled diiron(III) cluster, ferrous soaking involves adding Fe(II) ions to the apo protein. Although the iron binding constants of the two sites have not been measured, Mössbauer spectroscopic studies on R2-wt indicate that one site, proposed to be the Fe2 site, has a significantly greater affinity for Fe(II).[59] In support of this conclusion, only the Fe2 site is occupied in the crystal structure of mouse R2.[60] The geometry at the mouse Fe2 site is distorted octahedral with the Fe(II) ion coordinated by Glu 170, Glu 233, Glu 267, and His 270, which correspond to *E. coli* Glu 115, Glu 204, Glu 238, and His 241, respectively. Notably, Glu 267 is chelating to Fe2. If the *E. coli* Fe2 site is loaded before the Fe1 site in solution, then it may be that Glu 238 first chelates Fe2 just as Glu 267 does in the mouse protein, and then, upon loading of the Fe1 site, bridges the two iron ions in a $\mu$-($\eta^1$,$\eta^2$) fashion (Figure 1B). For chemical reduction of oxidized crystals, Glu 238 is initally a monodentate, terminal ligand to Fe2, and rearrangement to $\mu$-1,3 coordination may be more favorable (Figure 1C). A subsequent rearrangement step might then result in the $\mu$-($\eta^1$,$\eta^2$) bridge observed in the ferrous soaked form (Figure 1B). Computational studies indicate that this rearrangement should be facile with an activation barrier of only a few kcal/mol.[61] The barrier to this rearrangement may be greater in the crystal than in solution, trapping the dithionite or photoreduced diiron(II) site with Glu 238 in the $\mu$-1,3 geometry. It is interesting that Glu 238 adopts an intermediate geometry in one monomer of the R2-wt pH 5 structure. Rearrangement in the

(57) Eriksson, M.; Jordan, A.; Eklund, H. *Biochem.* **1998**, *37*, 13 359−13 369.
(58) Högbom, M.; Huque, Y.; Sjöberg, B.-M.; Nordlund, P. *Biochem.* **2002**, *41*, 1381−1389.
(59) Bollinger, J. M., Jr.; Chen, S.; Parkin, S. E.; Mangravite, L. M.; Ley, B. A.; Edmondson, D. E.; Huynh, B. H. *J. Am. Chem. Soc.* **1997**, *119*, 5976−5977.
(60) Kauppi, B.; Nielsen, B. B.; Ramaswamy, S.; Larsen, I. K.; Thelander, M.; Thelander, L.; Eklund, H. *J. Mol. Biol.* **1996**, *262*, 706−720.
(61) Torrent, M.; Musaev, D. G.; Morokuma, K. *J. Phys. Chem. B* **2001**, *105*, 322−327.

crystal between the $\mu$-1,3 and $\mu$-($\eta^1$,$\eta^2$) coordination modes may be more facile for this subunit at low pH.

It appears that the situation is precisely reversed in variants with the D84E substitution: the structure of the diiron(II) protein prepared by ferrous soaking has the $\mu$-1,3 coordination by Glu 238 (Figure 3B) observed in dithionite-reduced and photoreduced R2-wt (Figure 1D), whereas the previously reported structure of the dithionite-reduced form of R2-D84E has the $\mu$-($\eta^1$,$\eta^2$) coordination (Figure 3C) observed in ferrous soaked R2-wt (Figure 1B). According to the above arguments, this reversal could, in principle, reflect a reversal in the rank order of affinities of the Fe1 and Fe2 sites. The relative affinities of the two sites in R2-D84E have not been determined (and, in fact, cannot be determined by the same approach applied to R2-wt, due to the fact that the D84E substitution abolishes the Mössbauer spectroscopic resolution between the two sites of the product diiron(III) cluster). Nevertheless, crystal structures of R2-D84E and R2-D84E/Y122F with only the Fe2 site occupied have been obtained,[62] suggesting that this site has the greater affinity for Fe(II) even with the D84E substitution present. It seems more likely that the reversal in the coordination modes of Glu 238 in ferrous soaked and dithionite-reduced R2-D84E relative to the cognate forms of R2-wt relates to a similar reversal in the coordination mode of the residue 84 carboxylate ligand. In both forms of diferrous R2-wt, Asp 84 is monodentate to Fe1 (Figure 1). By contrast, Glu 84 is, in all structures determined for the diiron(II) form of R2-D84E (as well as in structures of all "double mutants" containing the D84E substitution), bidentate chelating (Figure 3B,C), and swings away to a monodentate position upon conversion to the diiron(III) state.[30]

A final difference between the two procedures is the composition of the soaking and cryosolutions. Previous studies of both R2 and sMMO suggest that the diiron center is sensitive to solvent effects. For sMMO, the diiron(III) center in crystals soaked in 10% DMSO exhibits altered coordination for two of the carboxylate ligands.[63] For diferric R2, Asp 84 is symmetrically bidentate, chelating in the 2.2 Å resolution structure,[26] but monodentate in the 1.4 Å resolution cryo structure.[64] This difference could be due to the soak in glycerol-containing cryosolution prior to freezing, but might also be attributed to the use of much higher resolution data in the crystallographic refinement. Notably, high concentrations of glycerol have been observed to affect metal loading of R2.[65] Because both the chemically reduced[28] and ferrous soaked crystals are frozen in a cryosolution containing 20% glycerol, such solvent effects are unlikely to account for the observed structural differences. It is possible that excess ferrous ammonium sulfate could influence the geometry of the ferrous soaked diiron(II) center. There is, however, no evidence in the electron density maps for bound ions or global structural changes due to interaction with such ions. Therefore, we favor the proposal that differences in the initial structures in the crystal, rather than pH or solvent effects, lead to the observed differences at the diiron(II) site.

**Comparison to CD and MCD Spectroscopic Data**. An unresolved issue from previous studies of diferrous *E. coli* R2 is a discrepancy between coordination geometries determined by X-ray crystallography and CD/MCD spectroscopy. The CD and MCD spectra show two low energy transitions at ~5500 $cm^{-1}$ and ~7000 $cm^{-1}$ and one high energy band at ~9000 $cm^{-1}$, indicating that the two Fe(II) ions have different coordination environments. The transitions are best interpreted as arising from one five-coordinate Fe(II) with distorted trigonal bipyramidal geometry and one distorted tetrahedral four-coordinate Fe(II). The two Fe(II) ions are weakly antiferromagnetically coupled.[41] The diiron(II) cluster obtained in the crystal by either chemical reduction or photoreduction contains two four-coordinate Fe(II) ions, however (Figure 1C).[28] There are several possible explanations for this inconsistency.[2] First, Glu 204, assigned as monodentate in the crystal structure, could be bidentate, rendering Fe2 five-coordinate. Although it is clearly monodentate in one subunit with Fe2···O distances of 2.17 and 2.88 Å, the second subunit is more ambiguous with Fe···O distances of 2.44 and 2.50 Å.[28] Second, a solvent ligand not detected in the electron density could be present. Finally, the high concentrations of glycerol (>50%) in the CD/MCD samples[41] could result in a different geometry. Given that the chemically reduced and ferrous-soaked crystals were treated with the same 20% glycerol-containing cryosolutions, this scenario seems unlikely.

The structures reported herein suggest a third possibility: the solution form studied by CD/MCD spectroscopy and the crystalline, dithionite, or photoreduced proteins could have different diiron(II) cluster structures. The crystal structure of ferrous soaked R2-wt (Figure 1B) is more consistent with the CD/MCD data than the structures reported for the dithionite and photoreduced forms. Fe1 is four-coordinate and Fe2 is five-coordinate, although the $\mu$-($\eta^1$,$\eta^2$) bridging mode of Glu 238 might be expected to result in ferromagnetic coupling.[41,66] The observed antiferromagnetic coupling could be attributable to asymmetric coordination of the bridging oxygen. Although the Fe···O distance is 2.4 Å for both Fe(II) ions in one subunit in the dimer, the Fe···O distances in the second subunit are 2.2 and 2.5 Å for Fe1 and Fe2, respectively. The ferrous soaked complex, rather than the complex generated in crystals by chemical or photoreduction, may therefore represent the species present in the CD/MCD samples. In the spectroscopic studies, it was verified that chemical reduction and addition of ferrous ions to apo protein give rise to indistinguishable forms.[41,66] The simplest explanation is that conversion of the form initially generated by chemical or photoreduction to the ferrous soaked form is facile in solution but kinetically hindered in the crystal.

The above hypotheses also can accommodate data on binding of azide to the diiron(II) cluster of R2-wt and site-directed variants. CD/MCD data indicate that a single azide ion binds to the five-coordinate Fe(II) ion in R2-wt, yielding one six-coordinate and one four-coordinate site.[41] The data further suggest that the two sites are minimally perturbed, other than by the binding of the exogenous ligand. The crystal structure of chemically reduced R2-Y122F/F208A with $N_3^-$ bound is

(62) Sommerhalter, M.; Voegtli, W. C.; Bollinger, J. M., Jr.; Rosenzweig, A. C., unpublished results.
(63) Rosenzweig, A. C.; Frederick, C. A.; Lippard, S. J. In *Microbial Growth on $C_1$ Compounds: Proceedings of the 8th International Symposium*; Lidstrom, M. E., Tabita, F. R., Eds.; Kluwer Academic Publishers: Dordrecht, 1996; pp 141−149.
(64) Högbom, M.; Galander, M.; Andersson, M.; Kolberg, M.; Hofbauer, W.; Lassmann, G.; Nordlund, P.; Lendzian, F. *Proc. Natl. Acad. Sci. U.S.A.* **2003**, *100*, 3209−3214.
(65) Pierce, B. S.; Elgren, T. E.; Hendrich, M. P. *J. Am. Chem. Soc.* **2003**, *125*, 8748−8759.
(66) Wei, P.-P.; Skulan, A. J.; Mitic, N.; Yang, Y. S.; Saleh, L.; Bollinger, J. M., Jr.; Solomon, E. I. *J. Am. Chem. Soc.*, in press.

consistent with this analysis: Fe1 is four-coordinate, and Fe2 is six-coordinate with azide bound in an $\eta^1$-terminal fashion and Glu 238 in the $\mu$-($\eta^1$,$\eta^2$) coordination mode.[29] The structure of the chemically reduced protein in the absence of azide shows two four coordinate Fe(II) sites with Glu 238 in the $\mu$-1,3 coordination mode, however. Thus, binding of $N_3^-$ would, according to the structural data, have to induce a shift of Glu 238 to the $\mu$-($\eta^1$,$\eta^2$) geometry. This shift is inconsistent with the CD/MCD spectroscopic results which suggest minimal perturbation to the bridging environment upon binding of one azide ion. The discrepancy is rectified if it is again assumed, as has been argued above for R2-wt, that the diiron(II) cluster of the chemically reduced R2-Y122F/F208A remains trapped in the crystal in the coordination geometry that is disfavored in solution (with Glu 238 in the $\mu$-1,3 mode). According to this hypothesis, binding of azide drives the shift in the crystal to the preferred configuration (with Glu 238 in the $\mu$-($\eta^1$,$\eta^2$) mode). In solution, the preferred configuration is already present, and binding of $N_3^-$ can occur with minimal rearrangement. It should be noted, however, that the single azide adduct observed by CD/MCD exhibited antiferromagnetic coupling, which may not be consistent with Glu 238 adopting $\mu$-($\eta^1$,$\eta^2$) geometry.[41,66]

The diferrous forms of R2-D84E and R2-D84E/W48F have also been studied by CD and MCD spectroscopies.[66] Spectra indicate the presence of one four-coordinate and one five-coordinate Fe(II) ion in the clusters of both variants. This interpretation is completely consistent with the structures of ferrous soaked R2-D84E and R2-D48E/W48F in which Fe1 is five-coordinate and Fe2 is four-coordinate (Figures 2B,C, 3B). For R2-D84E, samples prepared by chemical reduction and by addition of Fe(II) to the apo protein gave identical results.[66] By contrast, the Fe(II) ions are five-coordinate and six-coordinate in dithionite-reduced R2-D84E (Figure 3C). There is no evidence for six-coordinate Fe(II) in the CD/MCD spectra of R2-D84E.[66] These comparisons suggest that the diiron(II) clusters present in the ferrous soaked R2-D84E and R2-D84E/W48F crystals probably have the same coordination as the clusters formed in solution by either chemical reduction or ferrous soaking, whereas dithionite reduction of R2-D84E crystals leads to trapping of a structurally distinct diiron(II) cluster.

**Mechanistic Implications.** The differences between the structures reported herein of the ferrous soaked R2 proteins and the previously reported structures of dithionite and photoreduced forms suggest that the latter may not necessarily represent the preferred conformation of the diiron(II) cluster in solution. The structures of the ferrous soaked proteins provide alternative and perhaps more appropriate starting points for consideration of possible $O_2$ activation mechanisms. On the basis of the structure of the R2-F208A/Y122F azide adduct, Nordlund and co-workers suggested that $O_2$ binding induces a shift in Glu 238 from the $\mu$-1,3 to the $\mu$-($\eta^1$,$\eta^2$) bridging conformation.[29] In their proposed mechanism, Glu 238 retains this conformation during formation of a peroxodiiron(III) intermediate, decomposition of this intermediate by O−O bond cleavage, and electron transfer to yield intermediate **X**. Upon oxidation of Tyr 122 and formation of the product diiron(III) cluster, Glu 238 swings away to become monodentate only to Fe2. If the initial structure of diferrous R2-wt assumed in Nordlund's mechanistic scheme (that of the dithionite-reduced form) is replaced with the structure of ferrous soaked R2-wt determined here, then no conformational changes in Glu 238 would accompany $O_2$ binding or intermediate formation. The absence of major conformational changes in the carboxylate ligands would be consistent with the fast, second-order kinetics ($k = 2 \times 10^5$ $M^{-1}s^{-1}$) with which the diiron(II) form of the protein reacts with $O_2$.[22]

Whereas it is unclear whether a peroxodiiron(III) complex similar to MMOH **P** is an intermediate in the reaction of R2-wt, such a species accumulates to high levels in the reactions of both the R2-D84E[24] and R2-D84E/W48F[25] variants. Resonance Raman data indicate that this species is a symmetric $\mu$-1,2-peroxodiiron adduct.[25] The D84E substitution thus either stabilizes the peroxo intermediate relative to the same adduct in R2-wt or causes it to form in preference to a chemically distinct and more reactive species that forms in R2-wt.[30] Until these two possibilities can be distinguished, it is difficult to use structural data to rationalize the accumulation of the peroxo species in the variant proteins but not R2-wt. Moreover, the structure of dithionite-reduced R2-D84E (Figure 3C) differs from that of ferrous soaked R2-D84E (Figure 3B) and R2-D84E/W48F. Both Glu 204 and Glu 238 adopt different coordination geometries in the latter proteins than in dithionite-reduced R2-D84E. However, there is one important similarity. In all of the structures with the D84E substitution, Glu 84 is chelating to Fe1 (Figure 3), whereas in all structures of diiron(II) R2-wt, Asp 84 is a monodentate, terminal ligand to Fe1 (Figure 1). As a result of the altered position of Glu 84, a hydrogen bond linking the uncoordinated oxygen of Asp 84 with the side chain hydroxyl group of Tyr 122 in diferrous R2-wt is not present in the D84E variant proteins. The structure of Mn-substituted R2-D84E (Figures 2D, 3D) is very similar to that of ferrous soaked R2-D84E, and recapitulates the conformational changes at residue 84.

These observations suggest that attempts to relate the known mechanistic differences to structure should focus on the coordination geometry of Asp and Glu 84. Most proposed mechanisms for the reaction are based on the MMOH reaction cycle and invoke a $\mu$-1,2-peroxodiiron(III) intermediate.[2,25,29,67] In most of these mechanisms, this species undergoes O−O bond cleavage to form an diiron(IV) intermediate analogous to MMOH **Q**, and this step is followed by electron transfer (now known to occur from Trp 48) to the cluster to generate **X**. It should be noted, however, that no evidence for a **Q**-like intermediate in the R2 reaction pathway has been obtained. ENDOR spectroscopic data suggest that the two oxygen atoms from $O_2$ are present in **X** as an oxo bridge and a terminal aqua ligand.[68] If the detailed mechanism recently proposed by Nordlund and co-workers[29] is considered with the structure of ferrous soaked R2-wt as the starting point (Figure 1B), then addition of $O_2$ in $\mu$-1,2 fashion with minimal ligand rearrangement would render Fe1 five-coordinate and Fe2 six-coordinate. Dioxygen cleavage and formation of **X** would then result in a bridging oxo and a terminal aqua ligand bound to Fe1. For ferrous soaked R2-D84E (Figure 3B), addition of $O_2$ would render Fe1 six-coordinate and Fe2 five-coordinate in the $\mu$-1,2-peroxodiiron(III) intermediate. For a terminal aqua ligand to be accommodated on Fe1, a rearrangement would be necessary.

A likely participant in such a rearrangement is Glu 84 itself. In the structure of oxidized R2-D84E, Glu 84 is a monodentate,

(67) Stubbe, J.; Donk, W. A. v. d. *Chem. Rev.* **1998**, *98*, 705−762.
(68) Burdi, D.; Willems, J.-P.; Riggs-Gelasco, P.; Antholine, W. E.; Stubbe, J.; Hoffman, B. M. *J. Am. Chem. Soc.* **1998**, *120*, 12 910−12 919.

terminal ligand,[30] suggesting that one of the coordinated oxygen atoms is displaced during oxygen activation. Although density functional studies predict that the monodentate and bidentate coordination modes are close in energy,[61] the conversion of Glu 84 from bidentate to monodentate could constitute a rate-limiting step in the R2-D84E $O_2$ activation mechanism, allowing for accumulation of the observed $\mu$-1,2-peroxodiiron(III) species and suppressing accumulation of **X**. Alternatively, if the canonical $\mu$-1,2-peroxodiiron(III) complex is not part of the R2-wt reaction pathway, the differences in coordination geometry resulting from the D84E substitution might also explain its formation in the variant proteins. As discussed previously, a superoxo intermediate might precede **X** in the R2-wt mechanism.[30] In one possible scenario, superoxide coordinates to Fe1 in an $\eta^2$ fashion. The four-coordinate Fe1 site in R2-wt (Figure 1B,C) could accommodate such a geometry, whereas the five-coordinate Fe1 site in R2-D84E (Figure 3B,C) might preclude formation of this species and instead favor the observed addition of $O_2$ in $\mu$-1,2 fashion.

**Conclusions.** Crystal structures of the diiron(II) forms of *E. coli* R2-wt and its D84E and D84E/W48F variants determined from crystals of apo protein soaked with ferrous ions reveal active site geometries different from those obtained by chemical or photoreduction of iron-loaded oxidized crystals. Structures of R2-wt and R2-D84E/W48F determined at pH 7.3 and at pH 5 suggest that these differences cannot be attributed solely to pH effects. These structures of ferrous soaked R2 finally resolve discrepancies between CD/MCD data and previously reported structures. The $O_2$ activation mechanism can now be considered with these structures, which may represent the actual diiron(II) cluster structure in solution, as starting points. In particular, future computational studies should benefit from this newly expanded set of reduced R2 structures.

**Acknowledgment.** This work was supported by funds from the David and Lucile Packard Foundation (A.C.R.) and by NIH grant GM55365 (J.M.B.). W.C.V. was supported in part by NIH Training Grant GM08382. The SSRL Structural Molecular Biology Program is supported by the Department of Energy, Office of Biological and Environmental Research, and by the National Institutes of Health, National Center for Research Resources, Biomedical Technology Program, and the National Institute of General Medical Sciences. The Advanced Light Source is supported by the Director, Office of Science, Office of Basic Energy Sciences, Materials Sciences Division, of the U.S. Department of Energy under Contract No. DE-AC03-76SF00098 at Lawrence Berkeley National Laboratory. We thank R. Lieberman for assistance with figure preparation.

JA0370387